

ある。

2. ヒトにおけるレプチン

ヒトにおけるレプチンの変異は、重症でかつ若年発症の肥満との密接な関連が報告されているが、このような遺伝子変異が認められる例はまれである。しかしながら、ほとんどのヒト肥満例で血中レプチン値の上昇を認め、レプチン抵抗性がヒトにおける肥満発症機序に重要な役割を担っている可能性が示唆されている。また、レプチン産生は、血中のグルコースや脂肪酸、性ホルモン、副腎皮質ステロイドなど多くの要素に影響されるが、血中インスリン値とも相関することが明らかにされている²⁾。

3. レプチン受容体

レプチンの生体内での代表的な効果は、視床下部ニューロンのレプチン受容体を経て発現されることが知られているが、レプチン受容体は視床下部のみならず副腎皮質、膵臓のβ細胞やTリンパ球、消化管、そして肝臓などの臓器にも存在することが明らかにされた。

レプチン受容体は、クラスIサイトカインレセプターファミリーに属し、IL-6受容体と多くの共通点を有する。また、レプチン受容体は、long isoform(OB-Rb)とshort isoform(OB-Ra)に分けられ、long isoform(OB-Rb)がシグナル伝達には重要な役割を担っているとされる。他方、short isoform(OB-Ra)は多くの臓器に発現しているが、生物学的な意義は不明な点が多い。

肝臓内では、肝細胞、Kupffer細胞、内皮細胞などに存在するとされているが最近、星細胞でもその存在が明らかにされた。しかし、Kupffer細胞、内皮細胞では重要とされ

る long isoform(OB-Rb)の発現を認めているのに対し、星細胞では short isoform(OB-Ra)の発現を報告したものと³⁾、long isoform(OB-Rb)の発現を確認した報告がある⁴⁾。レプチンのシグナル伝達は受容体結合後、Jak-Stat系を介して標的遺伝子を活性化すると考えられている。

II. レプチンと NASH

1. NASHの原因と経緯

NASHは脂肪肝を背景に実質の壊死・炎症や線維化の所見がみられる病態を指す。臨床統計上にも示されるように、NASHの主たる原因は肥満(とくに中心性肥満)とインスリン抵抗性であるといわれている。肥満・インスリン抵抗性のある状態から脂肪肝を経てNASHへ至る過程には、脂肪蓄積と炎症・線維化という二つの異なるステップがある。脂肪肝はNASHの前段階ではあるが、脂肪肝そのものが炎症・線維化のすべての原因ではない。脂肪肝の多くは進行性ではなく、一部に酸化ストレスなど、なんらかの二次的刺激(second hit)が加わってはじめて炎症・線維化が誘導されると考えられる。

すなわち、第一段階としてインスリン抵抗性と血中インスリン濃度上昇を背景として、肝細胞内ミトコンドリアでのβ酸化をインスリンが阻害し、肝細胞内の脂肪酸濃度が上昇する。さらにインスリン抵抗性は、脂肪酸の肝臓への輸送を増加させ、結果的に余剰の中性脂肪が肝細胞内に蓄積すると考えられている⁵⁾。

第二段階(second hit)としては酸化ストレスが考えられている。すなわち、脂肪酸によりcytochrome P 450 2E1が誘導され、内因性のケトン、アルデヒドや外来性のN-ニ

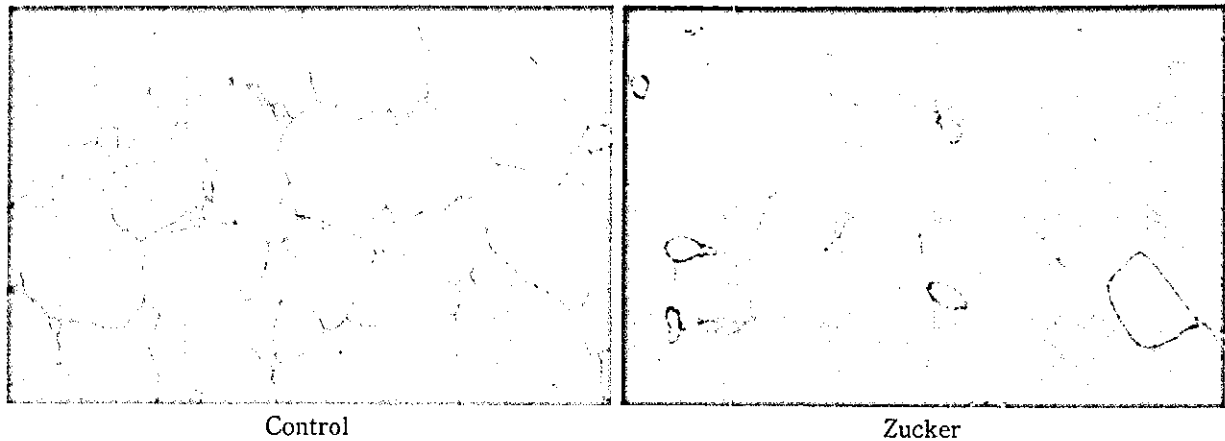


図1 Sirius red 染色
Zucker およびそのコントロールラットにブタ血清を8週間投与し、線維化を Sirius red 染色した。Zucker ラットでは明らかに線維化が抑制されていた。

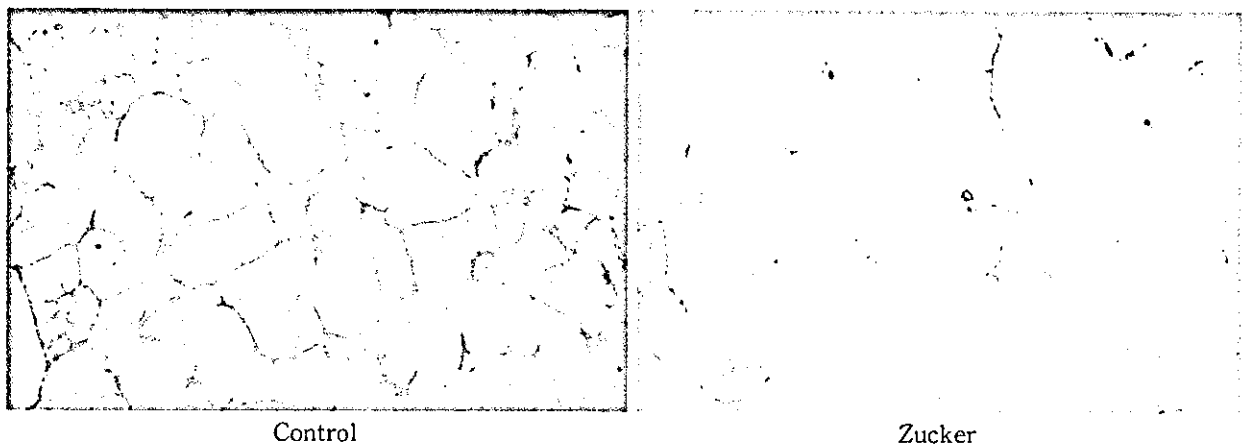


図2 アルファー平滑筋アクチン染色
図1の組織で活性化星細胞の指標であるアルファー平滑筋アクチンを染色したところ、Zucker ラットでは明らかに活性化星細胞数が抑制されていた。

トロソアミンの代謝過程で活性酸素が発生し、肝障害が誘発される。この障害が、炎症細胞浸潤を惹起し Kupffer 細胞や脂肪組織からの TNF- α などの炎症性サイトカインの過剰産生が引き起こされ、壊死・炎症や線維化が進行するものと考えられている。

2. レプチンとの関わり

近年、レプチンが隣 β 細胞でのインスリン分泌と組織におけるインスリン反応性の両方を調節していることが知られるようになってきた²⁾。肝細胞内において、レプチンはイ

ンスリン感受性に対し複雑な二面的役割を担う。レプチンは肝細胞内の輸送と代謝回転を促進し、これはインスリンの作用に補完的に働く一方で、レプチンは IRS-1 に代表される細胞内シグナル蛋白のインスリン惹起性のリン酸化に対し抑制的に、また糖新生についてはダウンレギュレートする方向に作用する。このことからレプチンはインスリン抵抗性の発現を促している可能性が示唆される²⁾。したがって、ヒトにおける肥満に伴った血中レプチン濃度の上昇は、インスリン抵抗性と血中インスリン濃度の上昇を促進し、

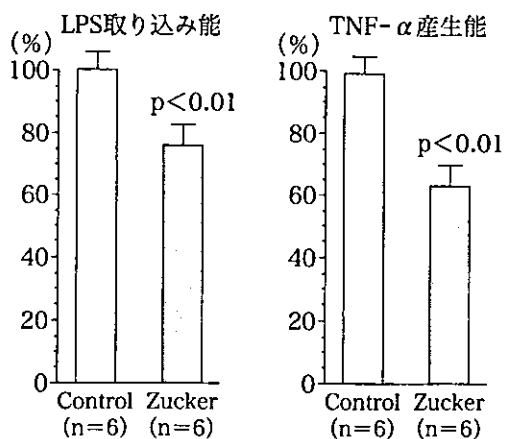


図3 Kupffer細胞機能の比較

Zucker およびそのコントロールラット (normal) からの分離 Kupffer 細胞における, FITC-LPS 取り込みと TNF- α 産生を比較検討した。いずれも Zucker ラットで有意に抑制されていた。

そして肝細胞内のインスリンシグナル伝達を変化させて肝細胞内に脂肪酸を蓄積させるという、二つの側面から肝臓の脂肪化に寄与していると考えられている。

3. レプチンと基礎研究—肝線維化に関する検討

レプチンと肝線維化の関連性を検討した教室のデータを紹介する。

1) Zucker ラットの Kupffer 細胞における検討

レプチンレセプターの遺伝子に変異し、レプチンのシグナルが伝達されず、肥満を引き起こす Zucker ラットを用いて検討した。この Zucker ラットおよびそのコントロールラットにブタ血清を腹腔内に週 2 回 8 週間投与し、線維肝を作製した。その結果、図 1 に示すように Zucker ラットでは、コントロールに比べて有意に線維化は抑制され、しかも活性化星細胞(アルファー平滑筋陽性細胞)の数も減少していた(図 2)。そこで、Zucker ラットおよびコントロールラットからそれぞれ

れ、Kupffer 細胞を分離培養し、LPS の取り込み能と TNF- α 産生能を比較検討した。その結果、Zucker ラットの Kupffer 細胞では、LPS の取り込み能と TNF- α 産生能とも、コントロールの Kupffer 細胞に比べて、有意に抑制されていた(図 3)。

2) ブタ血清投与ラットの Kupffer 細胞における検討

われわれは、ブタ血清投与ラットより分離した Kupffer 細胞では、無刺激のラットの Kupffer 細胞より大量の TGF- β_1 を産生していることを確認している。すなわち、このモデルでは異種蛋白であるブタ血清を Kupffer 細胞が取り込み TGF- β_1 などのサイトカインを放出し、星細胞を活性化させ肝線維化を引き起こしていると考えている。ところが、レプチン受容体の変異した Zucker ラットでは、Kupffer 細胞の取り込み能が低下し、サイトカインの産生も減少し、星細胞の活性化が抑制されたと考えられる。星細胞の増殖・活性化に重要な血小板由来成長因子(PDGF)などの発現に Zucker ラットとコントロールラットの Kupffer 細胞で有意差があるかを今後明確にする必要がある。いずれにしろ、レプチンが Kupffer 細胞を介して肝線維化と密接に関連していることがわかった。

3) 星細胞とレプチンの関わり

他方、活性化した星細胞がレプチンを産生し⁶⁾、上記のように星細胞にレプチン受容体が存在することが明らかになった^{3),4)}。しかし、レプチンが autocrine 的に星細胞に作用しているかはまだ結論できない。Ikejima らは³⁾、肝臓内でのレプチンの標的細胞が内皮細胞と Kupffer 細胞であり、この細胞が産生した TGF- β_1 が星細胞を活性化させる経路を提唱している。また、TGF- β_1 ノックアウトマウスに肝障害を惹起しても星細胞の活性

化はあまり起こらないといった報告⁷⁾もある。先述のように Kupffer 細胞や内皮細胞が PDGF (あるいは未知のサイトカインなど) を出し、これが星細胞の活性化に関与するのではないかと考えられ今後の検討を要する。

さらにレプチン欠損マウスの腹腔マクロファージを使用した研究では、レプチンが IL-6, PGE₂ などの産生に関与していることも示されている⁸⁾。このように、レプチンは肝臓内において、単なる脂肪肝を炎症・線維化を伴う NASH へ進展させる重要な因子の一つである可能性が強い。

4. レプチンと臨床研究

こうした基礎研究のみならず、臨床研究面からもレプチンと肝障害の関係を示す報告が、近年になり数多くなされるようになった。NASH 患者において血中レプチン濃度の上昇がみられ、レプチン値は血中インスリン濃度や BMI, 体脂肪率と相関していたとの報告に加え、NASH 患者と慢性 C 型肝炎患者を比較した研究では、脂肪肝のない慢性 C 型肝炎、脂肪肝のある慢性 C 型肝炎、そして NASH の順に血中レプチンの値は高くなり、BMI も同様の傾向を示したという結果や血清レプチン濃度が高い C 型慢性肝炎患者がより線維化の頻度が高く、アルコール性肝障害患者においては予後が不良であることが知られている^{9),10)}。さらに、アルコール性の肝硬変症患者の血中レプチン濃度が高いことも報告されている¹¹⁾。こうした臨床統計上の種々のデータと基礎研究結果の双方から、レプチンが肝臓の炎症および線維化の進展に直接的または間接的であれ明らかに影響を及ぼしていると考えられている¹²⁾。

しかし、最近の報告の中には、NASH 患

者の血清中のレプチン濃度は、肝内の脂肪化とは相関するが、炎症・線維化の程度は必ずしも相関しないといったものがあり¹³⁾、結論を得るにはさらに時間が必要である。いずれにしろ肥満・インスリン抵抗性と脂肪肝ないし NASH の関連において、その病態を理解するうえでレプチンは注目を集めている。

おわりに

レプチンの作用は未だ完全には明らかにされていない点もあるが、この蛋白が NASH における肝臓の病態を規定する重要なサイトカインの一つであることは明らかであり、とくに肝硬変への進展のみならず発癌との関連性なども今後の検討課題である。

文 献

- 1) Zhang, Y., Proenca, R., Maffei, M., et al.: Positional cloning of the mouse obese gene and its human homologue. *Nature* 372; 425-432, 1994
- 2) Cohen, B., Novick, D. and Rubinstein, M.: Modulation of insulin activities by leptin. *Science* 274; 1185-1188, 1998
- 3) Ikejima, K., Takei, Y., Honda, H., et al.: Leptin receptor-mediated signaling regulates hepatic fibrogenesis and remodeling of extracellular matrix in the rat. *Gastroenterology* 122; 1399-1410, 2002
- 4) Saxena, N. K., Ikeda, K., Rockey, D. C., et al.: Leptin in hepatic fibrosis: evidence for increased collagen production in stellate cells and lean littermates of ob/ob mice. *Hepatology* 35; 762-771, 2002
- 5) James, O., Day, C.: Non-alcoholic steatohepatitis: another disease of affluence. *Lancet* 353; 1634-1636, 1999
- 6) Potter, J. J., Womack, L., Mezey, E., et al.: Transdifferentiation of rat hepatic stellate cells results in leptin expression. *Biochem. Biophys. Res. Commun.* 244; 178-182, 1998

- 7) Hellerbrand, C., Stefanovic, B., Giordano, F., et al. : The role of TGFbeta 1 in initiating hepatic stellate cell activation in vivo. *J. Hepatol.* 30 ; 77-87, 1999
- 8) Diehl, A. M. : Nonalcoholic steatosis and steatohepatitis IV. Nonalcoholic fatty liver disease abnormalities in macrophage function and cytokines. *Am. J. Physiol. Gastrointest. Liver. Physiol.* 282 ; G 1-5, 2002
- 9) Naveau, S., Giraud, V., Borotto, E., et al. : Excess weight risk factor for alcoholic liver disease. *Hepatology* 25 ; 108-111, 1997
- 10) Hourigan, L. F., Macdonald, G. A., Purdie, D., et al. : Fibrosis in chronic hepatitis C correlates significantly with body mass index and steatosis. *Hepatology* 29 ; 1215-1219, 1999
- 11) McCullough, A. L., Bugianesi, E., Marchesini, G., et al. : Gender-dependent alterations in serum leptin in alcoholic cirrhosis. *Gastroenterology* 115 ; 947-953, 1998
- 12) Marra, F. : Leptin and liver fibrosis : a matter of fat. *Gastroenterology* 122 ; 1529-1532, 2002
- 13) Chitturi, S., Farrell, G., Frost, L., et al. : Serum leptin in NASH correlates with hepatic steatosis but not fibrosis : a manifestation of lipotoxicity? *Hepatology* 36 ; 403-409, 2002

Summary

Leptin and NASH

Isao Sakaida* and Kiwamu Okita*

The discovery of leptin in 1994 represented a tremendous breakthrough in the field of obesity and the regulation of energy balance. Now, leptin is also known to be a regulatory factor influencing the immune system, insulin secretion, angiogenesis, wound healing and the pathophysiology of liver disease e. g. NASH (non-alcoholic steatohepatitis). NASH seems to develop as a progressive hepatic disease from fatty depositions in the liver. It is believed that this progression involves two steps. The first step is the accumulation of fatty acids, resulting in steatosis associated with insulin resistance strongly related to obesity. The mechanism of this first process involves oxidation of mitochondria' fatty acids, which are blocked by insulin. The second process leads to the occurrence of necrosis, inflammation and fibrosis. This involves oxidative stress by cytochrome P 450 2 E 1 induced with fatty acids. Due to this process, leptin should be added to the list of factors which may play crucial roles in the development of liver fibrosis. Stellate cells may be activated directly or indirectly by leptin with the interaction of Kupffer cells or endothelial cells. Clinical studies have also indicated that hyperleptinemia is a common finding in obese patients and this group of subjects has been shown to have a higher prevalence of fibrosis during chronic HCV infection and have worse prognoses for alcoholic liver disease.

Key words : Leptin, NASH, kupffer cell, stellate cell, TNF- α

**Department of Gastroenterology & Hepatology, Yamaguchi University School of Medicine, 1-1-1 Minamikogushi, Ube-city, Yamaguchi 755-8505, Japan*

A subpopulation of bone marrow cells depleted by a novel antibody, anti-Liv8, is useful for cell therapy to repair damaged liver

Naoki Yamamoto, Shuji Terai, Shinya Ohata, Tomomi Watanabe,
Kaoru Omori, Koh Shinoda, Koji Miyamoto, Toshiaki Katada,
Isao Sakaida, Hiroshi Nishina, and Kiwamu Okita



A subpopulation of bone marrow cells depleted by a novel antibody, anti-Liv8, is useful for cell therapy to repair damaged liver^{☆,☆☆}

Naoki Yamamoto,^a Shuji Terai,^{a,*} Shinya Ohata,^b Tomomi Watanabe,^b
Kaoru Omori,^a Koh Shinoda,^c Koji Miyamoto,^d Toshiaki Katada,^b
Isao Sakaida,^a Hiroshi Nishina,^b and Kiwamu Okita^a

^a Department of Molecular Science and Applied Medicine (Gastroenterology and Hepatology), Yamaguchi University School of Medicine, Minami Kogushi 1-1-1, Ube, Yamaguchi 755-8505, Japan

^b Department of Physiological Chemistry, Graduate School of Pharmaceutical Science, University of Tokyo, Hongo 7-3-1, Bunkyo, Tokyo 113 0033, Japan

^c Department of Neuro-anatomy and Neuroscience, Yamaguchi University School of Medicine, Minami Kogushi 1-1-1, Ube, Yamaguchi 755-8505, Japan

^d Department of Molecular Science and Applied Medicine (Kampo Medicine), Yamaguchi University School of Medicine, Minami Kogushi 1-1-1, Ube, Yamaguchi 755-8505, Japan

Received 2 December 2003

Abstract

We previously reported a new *in vivo* model named as “GFP/CCl₄ model” for monitoring the transdifferentiation of green fluorescent protein (GFP) positive bone marrow cell (BMC) into albumin-positive hepatocyte under the specific “niche” made by CCl₄ induced persistent liver damage, but the subpopulation which BMCs transdifferentiate into hepatocytes remains unknown. Here we developed a new monoclonal antibody, anti-Liv8, using mouse E 11.5 fetal liver as an antigen. Anti-Liv8 recognized both hematopoietic progenitor cells in fetal liver at E 11.5 and CD45-positive hematopoietic cells in adult bone marrow. We separated Liv8-positive and Liv8-negative cells and then transplanted these cells into a continuous liver damaged model. At 4 weeks after BMC transplantation, more efficient repopulation and transdifferentiation of BMC into hepatocytes were seen with Liv8-negative cells. These findings suggest that the subpopulation of Liv8-negative cells includes useful cells to perform cell therapy on repair damaged liver.

© 2003 Elsevier Inc. All rights reserved.

Keywords: Bone marrow cell; Cell therapy; Regenerative medicine; Hepatic stem cell; Migration; Transdifferentiation; Mesenchymal stem cell; Hematopoietic stem cell; Liver regeneration; Niche

Recently, several groups have reported the possible plasticity of bone marrow cells (BMCs) to transdifferentiate into a variety of non-hematopoietic cell lineages

[1–4]. Ever since the transdifferentiation of BMC into hepatocytes was documented following a bone marrow transplant from a man donor to a woman recipient [5,6],

[☆] **Abbreviations:** BMC, bone marrow cell; CCl₄, carbon tetrachloride; FAH, fumarylacetoacetate hydrolase; GFP, green fluorescent protein; EGFP, enhanced GFP; GFP-Tg mice, C57BL6/Tg14 (act-EGFP) OsbY01 mice; HSC, hematopoietic stem cell; E, embryonic day; MSC, mesenchymal stem cells; MAPC, multipotent adult progenitor cell.

^{**} This work was supported by Grants-in-Aid for Scientific Research from the Japan Society for the Promotion of Science (No. 13470121 to Shuji Terai, Isao Sakaida, and Kiwamu Okita, and No. 13770262 to Shuji Terai) for translational research from the Ministry of Health, Labor and Welfare (H-trans-5 to Shuji Terai, Isao Sakaida, Hiroshi Nishina, and Kiwamu Okita).

^{*} Corresponding author. Fax: +81-836-22-2240.

E-mail addresses: terais@yamaguchi-u.ac.jp (S. Terai), nishina@mol.f.u-tokyo.ac.jp (H. Nishina).

¹ Request for Anti-Liv8 contact to Dr. Hiroshi Nishina, Department of Physiological Chemistry, Graduate School of Pharmaceutical Science, University of Tokyo, Hongo 7-3-1, Bunkyo, Tokyo 113 0033, Japan.

BMC has been an attractive cell source in regenerative medicine because getting BMC is easier than obtaining other tissue-specific stem cells [7].

However, the results of recent studies have been mixed in that some studies found that BMC was hardly transdifferentiated while others documented high levels of transdifferentiation [8,9]. Successful transdifferentiation in cell therapy involves various cell and recipient factors, and these factors interact in a complex manner. Therefore, it is difficult to identify the conditions necessary for transdifferentiation, contributing to the varied results among past studies. A past study using a fumarylacetoacetate hydrolase (FAH) knockout mice (metabolic tyrosinemia model) showed that hepatic functions could be compensated by transplanting Lin-Kit+Sca+Thy1low (KTLS) marrow cells [10]. In the FAH model, KTLS cells form foci and transdifferentiate into hepatocytes. Results of recent studies suggest that KTLS cells transdifferentiate into hepatocytes due to fusion with hepatocytes [11,12]. The FAH model is a specialized model of metabolic liver damage, making it possible to analyze the transdifferentiation of BMC into hepatocytes and functional compensation. However, a model with which the transdifferentiation of BMC can be analyzed under conditions of more general liver damage is needed. Using autologous transplantation in GFP transgenic mice [13], we established an isogenic transplantation model to assess the transdifferentiation of BMC into hepatocytes. This model is unique in that uncultured BMCs efficiently migrate into the peri-portal area of the liver and transdifferentiate into immature hepatoblasts and differentiate into mature hepatocytes under the specific “niche” of persistent liver damage induced by persistent intraperitoneal administration of carbon tetrachloride (CCl₄) [14]. In this model, liver cirrhosis was induced by 4 weeks CCl₄ injection, and BMCs isolated from GFP transgenic mice were transplanted through the caudal vein. It is possible to chronologically observe colonization and transdifferentiation of BMC in the liver by continuous administration of CCl₄, and we have named this model as the “GFP/CCl₄ model.” Furthermore, in this model, as in the natural development of the liver, BMCs appear to be transdifferentiated into hepatoblasts and then into hepatocytes. In our GFP/CCl₄ model, the timing of cell transplantation and the state of recipients appear to be suitable for the transdifferentiation of BMC into hepatocytes. Cell transplantation and continuous liver damage made efficient transdifferentiation of BMC into hepatocytes. In a system similar to ours, human hematopoietic stem cells (HSCs) were transplanted into the bone marrow of immunologically tolerant NOD/SCID mice before administration of CCl₄, and these cells differentiated into albumin-positive hepatocyte-like cells after the CCl₄ administration [15]. These findings suggest that a special “niche” created by CCl₄-induced liver damage is im-

portant for the migration of BMC to the liver and transdifferentiation into hepatocytes. Also, it has been reported recently that CCl₄ administration is effective for improving the colonization of HSC to liver of NOD/SCID [16].

The liver functions as a metabolic organ, but during the fetal period, from embryonic day (E) 12 to 16 (E12–E16), the liver functions as a hematopoietic organ [17]. Several studies have reported that mesenchymal cells affect hepatic hematopoiesis during the fetal period [18,19]. After this hematopoietic period, hepatoblasts are involved in a complex manner to develop the liver as a metabolic organ. However, documentation of the existence of HSC in the adult liver suggests that, even in the adult liver, blood cells and hepatocytes still play some role in the maintenance of hepatic function [20]. To further analyze this aspect, we prepared new rat monoclonal antibodies using the fetal liver on E 11.5 as an antigen. One of these antibodies, anti-Liv2, specifically recognizes hepatoblasts in the fetal liver from E 9.5 to 12.5. The results of past studies using the anti-Liv2 antibody have shown that SEK1, a stress-signaling kinase, plays an important role in the proliferation of hepatoblasts, thus suggesting that inflammatory signals are involved in the proliferation of hepatoblasts [21].

Although various theories explain the existence of pluripotent stem cells in BMC, the exact composition of stem cells in BMC is not clear at this time; the following cell types are known to exist in bone marrow: HSC [4,10], side population cells [22], and mesenchymal stem cells (MSC) [23]. Although past studies used the existing antibodies and techniques, there have not been any studies based on the findings associated with natural liver development. Using fetal liver as an antigen, we prepared a new monoclonal antibody, anti-Liv8 antibody, to analyze which subpopulation of BMC could differentiate into hepatocytes under CCl₄-induced continuous liver damage in the GFP/CCl₄ model [14]. This anti-Liv8 antibody recognizes hematopoietic cells using a specific cell surface marker and it can be used to separate cells. In the present study, we used this new antibody to separate BMC of adult mice and then transplanted the different types into mice under identical conditions of the GFP/CCl₄ model to ascertain which types of BMCs transdifferentiate into hepatocytes.

Materials and methods

Mice. C57BL/6/Tg14 (act-EGFP) OsbY01 mice (GFP-Tg mice) showed GFP expression in multiple tissue and cells and were kindly provided by Masaru Okabe (Genome Research Center, Osaka University, Osaka, Japan) [13]. C57BL/6 female mice were purchased from Japan SLC (Shizuoka, Japan). AML1 knockout mice were generated

as described previously [24]. The genetic background of these mice used in this study was C57BL/6 mice. Male and female mice were mated overnight and female mice were scored based on vaginal plaques taken to represent E 0.5. Mice were anesthetized at the completion of experiments. All processes, including surgical steps, were undertaken with the guidance of the committee for animal and recombinant DNA experimentation at Yamaguchi University.

Production of rat monoclonal antibody, Liv8. Eight-week-old WKY/NCrj female rats were immunized in the hind footpads with 100 μ g E 11.5 murine fetal liver lysate in complete Freund's adjuvant (0.2 ml). Anti-Liv8 antibodies were raised according to a previously described protocol [21].

Immunohistochemical staining for fetal liver. Fetal liver at E11.5 was obtained from c57/BL/6 mice and AML1 knockout mice. Tissue preparation and immunohistochemical analysis were performed according to a previously described protocol [21]. We analyzed anti-Liv2- and anti-Liv8-positive cells in fetal liver.

Preparation of GFP-positive BMC. For isolation of BMC, GFP-Tg mice were sacrificed by cervical dislocation and the limbs were removed. GFP-positive BMCs were flushed from the medullary cavities of tibias and femurs with PBS culture solution using a 25 G needle. The cell solution was filtered through a cell strainer (16 μ m) to remove particular matter and centrifuged at 500g for 5 min. After centrifugation, the supernatant was removed and cells were resuspended to prepare 1.0×10^6 cells/ml GFP-positive BMC solutions. Preparation of BMC takes approximately 1.5 h.

FACS analysis of BMC using Liv8 antibody. Prepared GFP-positive BMCs were reacted with rat biotin anti-Liv8 IgG antibody, R-Phycoerythrin (R-PE)-conjugated rat anti-CD45 (leukocyte common antigen) monoclonal antibody (PharMingen, San Diego, USA) at the rate of 1 μ g per 10^6 total cells, mixed well, and incubated in the gobos for 30–40 min at 4 °C. Following the incubation with the first antibody, the cells were washed twice by 0.02 M PBS and centrifuged at 500g for 5 min. Labeled cells were then reacted to streptavidin–fluorescein isothiocyanate (FITC) conjugate (PharMingen) at the rate of 1 μ g per 10^6 total cells, mixed well, and incubated in the gobos for 30–40 min at 4 °C. After that, these were washed out once with 0.02 M PBS and centrifuged at 500g for 5 min. The labeled cells were analyzed using FACS Calibur (Becton–Dickinson).

Sort GFP positive BMC by Liv8 antibody. Prepared BMCs were reacted to rat anti-Liv8 IgG antibody at the rate of 1 μ g per 10^6 total cells, mixed well, and incubated in the gobos for 30–40 min at 4 °C. Then cells were washed two times by 0.02 M PBS and centrifuged at 500g for 5 min. Cells were labeled with rat anti-Liv8 IgG antibody by reacting with Goat Anti-Rat IgG MicroBeads (Miltenvi Biotec GmbH, Bergisch Gladbach, Germany) at the rate of 20 μ l per 10^7 total cells, mixed well, and incubated for 20–30 min at 4 °C. Labeled cells were washed once by 0.02 M PBS and centrifuged at 500g for 5 min. These cells were separated into Liv8-positive cells or negative cells by the Auto Magnetic Cell Sorting system (Auto MACS) (Miltenvi Biotec GmbH) for 10 min per tube.

Transplantation of Liv8-positive or negative BMC into persistent liver damaged mice. We developed a new in vivo model "GFP/CCl₄ model" for monitoring differentiation of BMCs into hepatocytes [14]. To generate a liver damage group, 0.5 ml/kg of CCl₄ was injected into the peritoneum of 6-week-old C57BL/6 females twice a week for 4 weeks. Liver cirrhosis resulting from the continuous injections of CCl₄ was confirmed. A control group of C57BL/6 mice that had not been treated with CCl₄ was also used. One day after the eighth injection, sorted Liv8-positive or Liv8-negative BMC (1×10^6 cells) was slowly injected into the caudal tail vein of mice using a 31 G needle and a Hamilton syringe. After transplantation, CCl₄ injections (0.5 ml/kg) were continued twice a week. Mice were sacrificed weekly up to 4 weeks.

Tissue preparation. The livers were thoroughly perfused via the heart with 4% paraformaldehyde (Muto, Tokyo, Japan). This step was crucial for washing out contaminating blood cells. For fixation, the perfused livers were incubated with 4% paraformaldehyde (Muto)

overnight and then soaked in 30% sucrose for a few more 3 days. Tissues were frozen in dry ice and then sectioned into 18- μ m slices using a cryostat (Moriyasu Kounetsu, Osaka, Japan) in preparation for dyeing.

Immunohistochemistry and double immunofluorescence for GFP. To avoid autofluorescence, we used immunostaining to assess the expression of GFP. Cells expressing GFP were analyzed by both fluorescent microscopy and conventional immunohistochemistry with anti-GFP antibody (Santa Cruz Biotechnology, Santa Cruz, California, USA). Immunohistochemical analysis was performed according to a previously described protocol [14,25]. Sectioned tissues were incubated with anti-GFP antibody (1:5000 FL, sc-8334; Santa Cruz Biotechnology), anti-albumin (1:5000, 55462; ICN Pharmaceuticals, Costa Mesa, CA, USA), and anti-Liv2 antibody (1:5000) [21]. For fluorescence immunohistochemistry, tissues were incubated with Alexa Fluor R 488 and 568 donkey anti-goat IgG(H + L) conjugate, Alexa Fluor R 488 goat anti-rabbit IgG(H + L) conjugate, and Alexa Fluor R 568 goat anti-rat IgG(H + L) conjugate (Molecular Probes, Eugene, OR) as secondary antibodies. Positive cells in the liver were quantified using a Provis microscope (Olympus, Tokyo, Japan) equipped with a charge coupled devise (CCD) camera and subjected to computer-assisted image analysis with MetaMorph software (Universal Imaging, Downingtown, PA). A total of 10 different areas per liver section were analyzed independently and the areas of positive cells were calculated using the MetaMorph software.

Serum albumin level analysis. Serum albumin levels during the 4 weeks after Liv8-positive or Liv8-negative BMC transplantation were analyzed using the SPOTCHEM EZ SP-4430 dry chemical system (Arkray, Kyoto, Japan).

Statistical analysis. Values are shown as means \pm SE. Data were analyzed by analysis of variance with Fisher's projected least significant difference test.

Results

Anti-Liv8 antibody detected hematopoietic progenitor cell in fetal liver at E 11.5

Previously we had raised a rat monoclonal antibody, anti-Liv2, which recognized hepatoblasts at E 9.5 [21]. As shown in Fig. 1A, Liv2-positive cells were also detected in fetal liver at E 11.5. Using the antibody developed in this study, Liv8-positive cells were seen in the fetal liver on E 11.5 (Fig. 1B). Fetal liver at E 11.5 functions as a secondary hematopoietic organ [17]. We analyzed whether anti-Liv8 positive cell is associated with hepatoblast or hematopoietic cell. We found Liv2-positive cells (Fig. 1C), but no Liv8-positive cells (Fig. 1D), in the fetal liver of AML1^{-/-} embryos which do not undergo definitive hematopoiesis [24]. These results suggested that anti-Liv-8 recognizes hematopoietic progenitor cell in fetal liver.

Liv8-positive cells exist in adult bone marrow and express CD45

Next, we investigated Liv8-positive cells in the BMC of adult GFP Tg mice. Liv8-positive cells were found to be present among adult BMCs in adult bone marrow when analyzed in GFP-Tg mice. We found around 32%

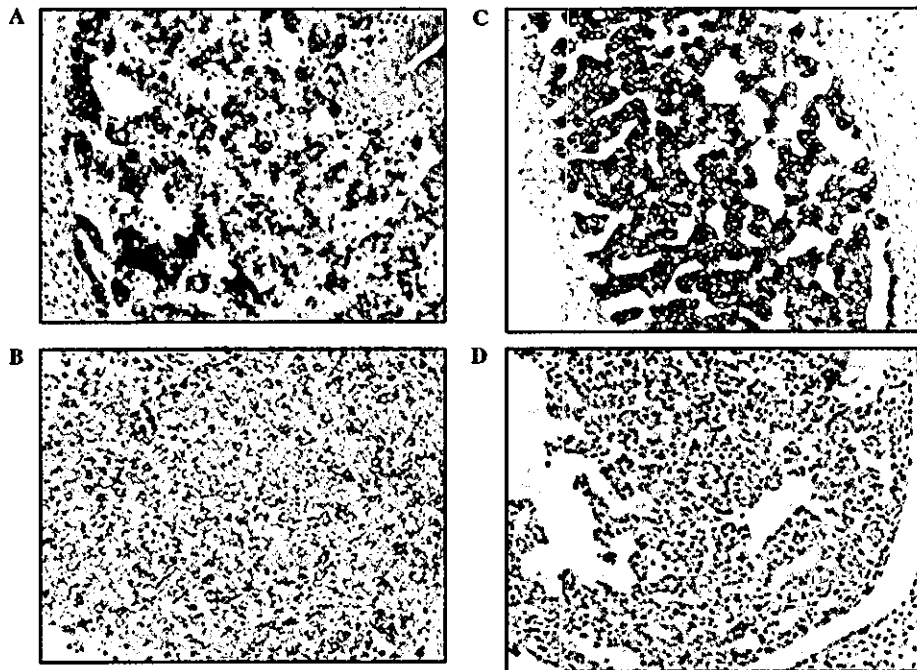


Fig. 1. (A–D) Liv2 and Liv8 expression at E 11.5 in normal and AML1^{-/-} mice. Liv2 (A,C) and Liv8 (B,D) expression at E 11.5 in normal fetal liver (A,B) and AML1^{-/-} mice (C,D). Magnification: (A–D) at 200 \times .

of Liv8-positive cells in adult GFP-Tg mice (Fig. 2A). We also analyzed the relationship between Liv8 and CD45, and found that 54% of Liv8-positive cells also

expressed CD45 (Fig. 2B). These results showed that anti-Liv8 is useful to separate hematopoietic cell and non-hematopoietic cell.

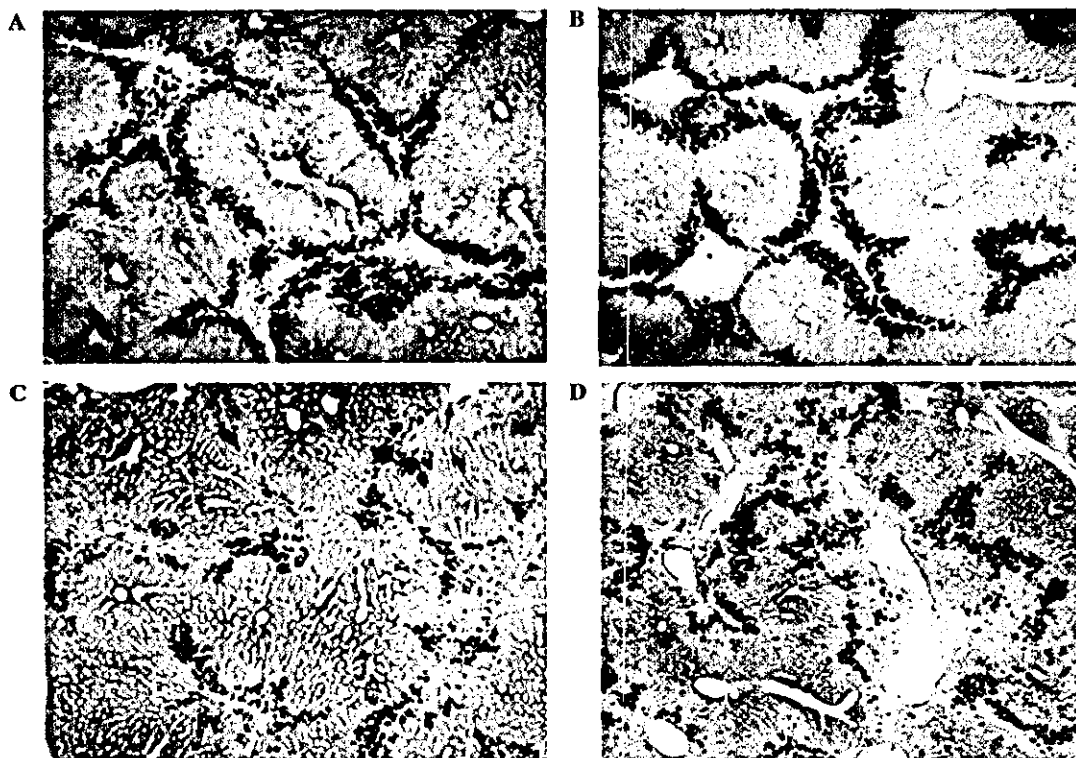


Fig. 3. (A–D) Expression of GFP in liver after transplantation of Liv8-positive and Liv8-negative cells. GFP expression in the liver after transplantation of Liv8-positive BMCs at 1 week (A) and 4 weeks (C), GFP expression at the liver after Liv8-negative BMC transplantation at 1 week (B) and 4 weeks (D) after cell injection. Magnification 200 \times .

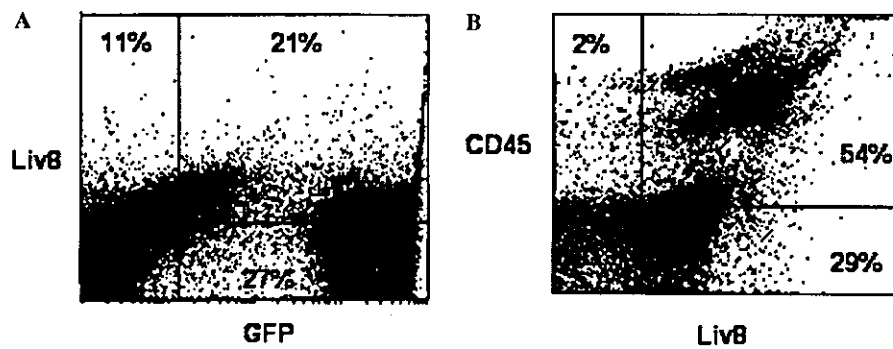


Fig. 2. Expression of CD45, Liv8 in bone marrow cell. FACS analysis of all BMCs of GFP-Tg mice. (A) Staining with Liv8 and GFP. (B) Staining with CD45 and Liv8.

Liv8-negative cells repopulated at the liver more than Liv8-positive cells

After separating Liv8-positive cells from Liv8-negative cells using AutoMACS, these cells were transplanted to recipient mice with CCl₄-induced liver cirrhosis. At one week after transplantation, both Liv8-positive (Fig. 3A) and Liv8-negative cells (Fig. 3B) colonized around the portal vein, with no marked differences in the rate of colonization (Table 1). In the Liv8-positive cell transplanted group, the number of GFP-positive cells in the liver increased transiently, but at four weeks after transplantation, the number of GFP-positive cells was significantly lower in the Liv8-positive cell group (Fig. 3C) than in the Liv8-negative cell group (Fig. 3D). Furthermore, GFP-positive cells were colonized inside the hepatic lobes in the Liv8-negative cell group at four weeks after transplantation. These results showed that Liv8-negative cell repopulated more than Liv8-positive cell.

The Liv8-negative cells transdifferentiate into hepatoblast phenotype

We showed in previous studies that transplanted BMCs transdifferentiate into Liv2-positive hepatoblasts and then further differentiate into hepatocytes [14,21]. In the present study, we also investigated the presence of cells expressing Liv2. Liv2-positive cells were identified by immunostaining, and the results showed that Liv2-

positive cells were seen around the portal region one week after transplantation, but that there was no significant difference in the number of Liv2-positive cells between Liv8-positive and Liv8-negative cell groups (Figs. 4A and B, and Table 1). With time, the number of Liv2-positive cells in the liver decreased significantly for the Liv8-positive cell group (Figs. 4C and D and Table 1). The transdifferentiation of myelogenic GFP cells into Liv2 cells was investigated. Cells that expressed both Liv2 and GFP were detected at four weeks after transplantation, and fluorescent staining showed that the expression of Liv2 by myelogenic cells was higher for the Liv8-negative cell group (Figs. 4E and F). These results indicated that Liv8-negative cell could be transdifferentiated into hepatoblast phenotype.

Albumin expression in the liver and serum albumin level following transplantation of Liv8-positive and Liv8-negative BMCs

At one week after cell transplantation, there was no marked change in the expression of albumin for both Liv8-positive and Liv8-negative cell groups (Figs. 5A and B). However, at four weeks after transplantation, the expression of albumin decreased with time for the Liv8-positive cell group (Fig. 5C), but remained the same for the Liv8-negative cell group (Fig. 5D). Furthermore, at four weeks after cell transplantation, the number of yellow cells expressing both albumin and GFP was higher for the Liv8-negative cell group

Table 1

Percent of area for each differentiation marker after Liv8(+) and Liv8(-) cell transplantation under the persistent liver damage

		1 week (n = 5)	2 weeks (n = 5)	3 weeks (n = 5)	4 weeks (n = 5)
GFP	Liv8(+)	11.1 ± 1.7	15.1 ± 2.1	9.4 ± 0.8	5.1 ± 0.6*
	Liv8(-)	11.7 ± 1.0	13.2 ± 0.8	12.4 ± 2.6	9.5 ± 3.6*
Liv2	Liv8(+)	6.0 ± 1.1	7.3 ± 3.5	8.2 ± 1.8	3.3 ± 0.9
	Liv8(-)	5.5 ± 1.3	5.8 ± 0.8	9.2 ± 0.6	7.7 ± 0.9
Albumin	Liv8(+)	15.0 ± 1.9	14.9 ± 2.5	6.8 ± 2.6*	3.7 ± 1.4*
	Liv8(-)	12.7 ± 3.2	12.5 ± 3.2	14.8 ± 1.3*	10.6 ± 2.1*

Values shown are percent of the area occupied.

*showed significant differences at each sampling point (n = 5) at $p < 0.05$ between Liv8(+) and Liv8(-) cell transplantation groups.

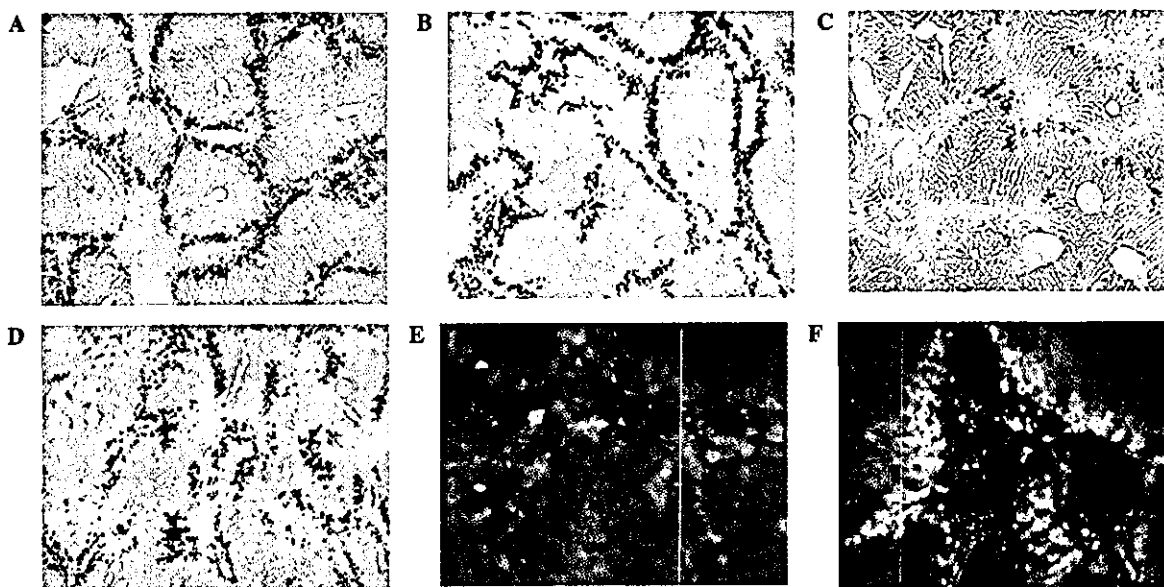


Fig. 4. (A–F) Expression of Liv2 antigen in liver after transplantation of Liv8-positive and Liv8-negative cells. Liv2 antigen expression at 1 week (A) and 4 weeks (C) after Liv8-positive BMC transplantation. Magnification at 200 \times . Liv2 antigen expression at liver at 1 week (B) and 4 weeks (D) after Liv8-negative BMC transplantation. Double fluorescent staining (red, Liv2; green, GFP; and yellow, Liv2 & GFP) of the liver at 4 weeks after Liv8-positive cell transplantation (E) and Liv8 negative cell transplantation (F) Magnification: (A–D) 200 \times , (E,F) 400 \times .

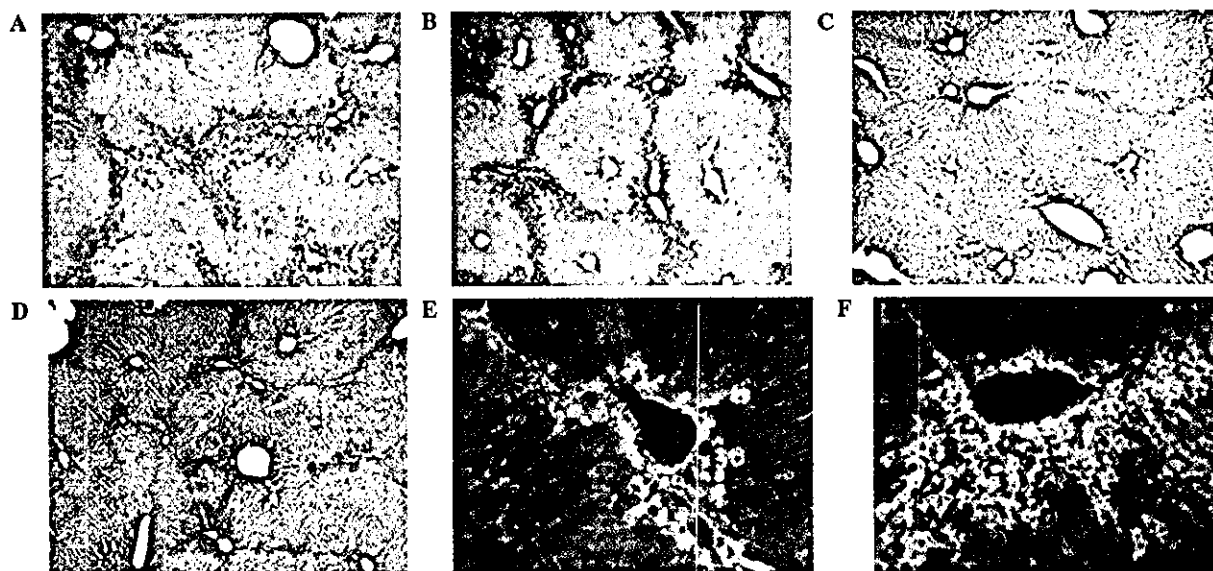


Fig. 5. (A–F) Expression Albumin after transplantation of Liv8-positive and Liv8-negative cells. Albumin expression at 1 week after transplantation of Liv8-positive cells (A) and Liv8-negative cells (B). Albumin expression at 4 weeks after transplantation of Liv8-positive cells (C) and Liv8-negative cells (D). Double fluorescent staining (red, albumin; green, GFP; and yellow, albumin & GFP) of liver at 4 weeks after transplantation of Liv8-positive cells (E) and Liv8-negative cells (F). Magnification: (A–D) 200 \times , (E,F) 400 \times .

(Figs. 5E and F). To ascertain whether transplanted cells were functioning as hepatocytes, serum albumin levels were measured. Serum albumin levels increased for both groups and were higher for the Liv8-negative cell group than the Liv8-positive cell group. The serum albumin levels at 4 weeks after Liv8-negative BMC transplantation showed the significantly higher levels for Liv8-negative cell group compared to the Liv8-positive BMC group ($n = 5$, $p < 0.05$) (Fig. 6). These results also

showed that Liv8-negative cell could transdifferentiate into albumin-positive hepatocyte.

Discussion

The anti-Liv8 antibody is a useful antibody to separate hematopoietic cells and non-hematopoietic cells in adult bone marrow. We found Liv8-positive cells in fetal

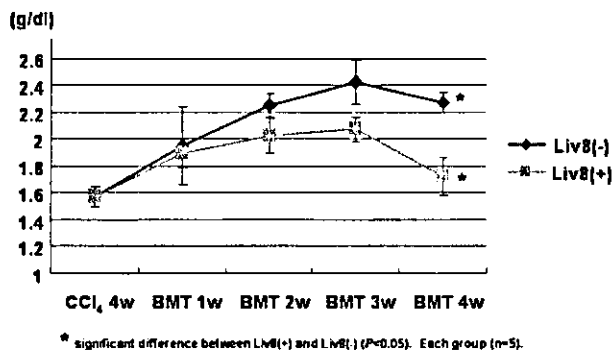


Fig. 6. The level of serum albumin. Serum albumin levels after Liv8-positive or Liv8-negative cell transplantation. CCl₄ 4w, 4 weeks CCl₄ injection group. BMT 1w, 1 week after BMC transplantation. BMT 2w, 2 weeks after BMC transplantation. BMT 3w, 3 weeks after BMC transplantation. BMT 4w, 4 weeks after BMC transplantation. * showed significant differences at each sampling point ($n = 5$) at $p < 0.05$.

liver at E11.5, but could not detect no-positive cells in fetal liver of AML1 knockout mice (Fig. 1C) at E 11.5. This result suggested that anti-Liv8-positive cell might be associated with the generation of HSC. We used FACS analysis to understand more about the characterization of Liv8-positive cells in the bone marrow. Around 32% of all BMCs, which were positive for Liv8, also expressed CD45 (Figs. 2A and B). CD45 is the pan-trophic marker for hematopoietic cell marker [26,27]. These results suggest that anti-Liv8 recognizes most hematopoietic cells. We separated BMCs into Liv8-positive cells and Liv8-negative cells using AutoMACS, and the repopulation and transdifferentiation of these cells into liver was analyzed in the GFP/CCl₄ model [14].

First we analyzed the colonization of transplanted Liv8-positive or negative cell. There was no change in the ratio of GFP-positive cells one week after transplantation between the Liv8-positive and Liv8-negative cell groups (Figs. 3A and B). In both groups, GFP-positive cells were found around the portal vein. The expression of GFP decreased with time for the Liv8-positive cell group (Fig. 3C), but in the Liv8-negative cell group, GFP-positive cells entered the hepatic lobes (Fig. 3D). At four weeks after transplantation, the rate of colonization for the Liv8-positive cell group was significantly lower than that for the Liv8-negative cell group (Table 1). Previously we found that colonization was not observed when BMCs were transplanted to normal recipients, but colonization was observed when BMCs were transplanted to recipients with liver cirrhosis caused by administration of CCl₄ [14]. Some previous studies also have reported that CCl₄ injection enhances the repopulation of hepatocytes following hepatocyte transplantation via the spleen [28,29]. It has been documented that elevated levels of SDF1 and

matrix metalloprotease 9 (MMP9) might have an important role for the migration of BMCs to the liver at liver damage by CCl₄ administration [16,30]. In the GFP/CCl₄, the expression of MMP9 was also increased by the transplantation of BMCs (I. Sakaida, unpublished data). At 1 week after transplantation, there was no marked difference in colonization between the Liv8-positive and negative transplantation groups. These results suggest that the early migration of BMC into liver was determined by the recipient condition. Next we analyzed the transdifferentiation of BMC into functional hepatocyte in the "niche" where transdifferentiation of BMC into hepatocyte is favorable [14]. The results of our past analyses have shown that transplanted BMCs transdifferentiate into Liv2-positive hepatoblasts and then differentiate into hepatocytes only under continuous inflammation. The persistent liver damage made by injection of persistent CCl₄ injection is important for the transdifferentiation of BMC [14]. When human HSCs were transplanted to immunologically tolerant NOD/SCID mice and followed up with administration of CCl₄, it was found that transplanted human HSC was differentiated into albumin express hepatocyte-like cell [15]. Albumin/promoter-Alb-DsRed2 Tg rat was established to monitor the transdifferentiation into albumin positive cell. Albumin-producing DsReds cell was increased by repeated administration of CCl₄ [31]. A study reported recently that the transdifferentiation of BMCs was low when inducing liver damage by CCl₄ administration before or after transplantation [32]. Different results were obtained with these systems because chronic liver damage before and after transplantation was not evident. The persistent liver damage might be the key factor to induce the transdifferentiation of BMC into hepatocyte. We investigated the transdifferentiation of Liv8 positive and negative BMCs into hepatoblast and hepatocytes by Liv2 and albumin expression. Like GFP, Liv2-positive cells were seen around the portal vein one week after transplantation for both Liv8-positive and Liv8-negative cell groups, and there was no marked difference between the two groups (Figs. 4A and B). On the other hand, at four weeks after transplantation, the expression of Liv2 for the Liv8-positive cell group was significantly lower than that for the Liv8-negative cell group (Figs. 4C and D). The results of double staining at four weeks after transplantation also showed that the number of myelogenic Liv2-positive cells was greater for the Liv8-negative cell group (Figs. 4E and F). Figs. 5C and D show the expression of albumin four weeks after transplantation and the expression of albumin for the Liv8-negative cell group was higher (Fig. 5D). The expression of albumin and GFP in myelogenic cells was significantly higher for the Liv8-negative cell group (Fig. 5F). Furthermore, we investigated functional recovery by comparing improvement in hepatic failure between the Liv8-positive and Liv8-negative cell groups.

As shown in Fig. 6, when CCl_4 was administered in the same manner to the Liv8-positive and Liv8-negative cell groups, and the level of serum albumin increased in both groups, but a significant finding in this analysis was significant improvements in the serum albumin levels at four weeks after transplantation in the Liv8-negative cell group compared to the Liv8-positive cell group ($p < 0.05$). These findings support those of immunostaining. These results can be summarized that Liv8-negative cells are more likely to transdifferentiate into hepatocytes with time passed. The subpopulation which was deleted by anti-Liv8 will be useful cells to use cell therapy using BMC to repair damaged liver. The Liv8 negative cell was thought to be non-hematopoietic cells. For example, multi-potent adult progenitor cells (MAPCs) from BMCs differentiate into functional hepatocyte like cells [33,34]. Our results might support that mesenchymal cells may differentiate into pluripotent cells under certain conditions.

Still the precise mechanisms to regulate repopulation and transdifferentiation BMC into hepatocyte are uncertain. To develop a cell therapy using BMC to repair damaged liver, we are planning to further analyze these mechanisms.

Acknowledgments

We thank Dr. Masaru Okabe (Genome Research Center, Osaka University) for the gift of GFP transgenic mice and Mr. Jun Oba for his excellent support for immunohistochemistry.

References

- [1] B.E. Petersen, W.C. Bowen, K.D. Patrene, W.M. Mars, A.K. Sullivan, N. Murase, S.S. Boggs, et al., Bone marrow as a potential source of hepatic oval cells, *Science* 284 (1999) 1168–1170.
- [2] N.D. Theise, M. Nimmakayalu, R. Gardner, P.B. Illei, G. Morgan, L. Teperman, O. Henegariu, et al., Liver from bone marrow in humans, *Hepatology* 32 (2000) 11–16.
- [3] M.R. Alison, R. Poulson, R. Jeffery, A.P. Dhillon, A. Quaglia, J. Jacob, M. Novelli, et al., Hepatocytes from non-hepatic adult stem cells, *Nature* 406 (2000) 257.
- [4] D.S. Krause, N.D. Theise, M.I. Collector, O. Henegariu, S. Hwang, R. Gardner, S. Neutzel, et al., Multi-organ, multi-lineage engraftment by a single bone marrow-derived stem cell, *Cell* 105 (2001) 369–377.
- [5] R. Okamoto, T. Yajima, M. Yamazaki, T. Kanai, M. Mukai, S. Okamoto, Y. Ikeda, et al., Damaged epithelia regenerated by bone marrow-derived cells in the human gastrointestinal tract, *Nat. Med.* 8 (2002) 1011–1017.
- [6] M. Korbling, R.L. Katz, A. Khanna, A.C. Ruifrok, G. Rondon, M. Albitar, R.E. Champlin, et al., Hepatocytes and epithelial cells of donor origin in recipients of peripheral-blood stem cells, *N. Engl. J. Med.* 346 (2002) 738–746.
- [7] S. Terai, N. Yamaoto, K. Omori, I. Sakaida, O. Kollet, A new cell therapy using bone marrow cells to repair damaged liver, *J. Gastroenterol.* 37 (Suppl. XIV) (2002) 162–163.
- [8] A.J. Wagers, R.I. Sherwood, J.L. Christensen, I.L. Weissman, Little evidence for developmental plasticity of adult hematopoietic stem cells, *Science* 297 (2002) 2256–2259.
- [9] E.L. Herzog, L. Chai, D.S. Krause, Plasticity of marrow-derived stem cells, *Blood* 102 (2003) 3483–3493.
- [10] E. Lagasse, H. Connors, M. Al-Dhalimy, M. Reitsma, M. Dohse, L. Osborne, X. Wang, et al., Purified hematopoietic stem cells can differentiate into hepatocytes in vivo, *Nat. Med.* 6 (2000) 1229–1234.
- [11] G. Vassilopoulos, P.R. Wang, D.W. Russell, Transplanted bone marrow regenerates liver by cell fusion, *Nature* 422 (2003) 901–904.
- [12] X. Wang, H. Willenbring, Y. Akkari, Y. Torimaru, M. Foster, M. Al-Dhalimy, E. Lagasse, et al., Cell fusion is the principal source of bone-marrow-derived hepatocytes, *Nature* 422 (2003) 897–901.
- [13] M. Okabe, M. Ikawa, K. Kominami, T. Nakanishi, Y. Nishimune, ‘Green mice’ as a source of ubiquitous green cells, *FEBS Lett.* 407 (1997) 313–319.
- [14] S. Terai, I. Sakaida, N. Yamamoto, K. Omori, T. Watanabe, S. Ohata, T. Katada, et al., An in vivo model for monitoring the transdifferentiation of bone marrow cells into functional hepatocytes, *J. Biochem. (Tokyo)* 134 (2003) 551–558.
- [15] X. Wang, S. Ge, G. McNamara, Q.L. Hao, G.M. Crooks, J.A. Nolte, Albumin-expressing hepatocyte-like cells develop in the livers of immune-deficient mice that received transplants of highly purified human hematopoietic stem cells, *Blood* 101 (2003) 4201–4208.
- [16] O. Kollet, S. Shvitiel, Y.Q. Chen, J. Suriawinata, S.N. Thung, M.D. Dabeva, J. Kahn, et al., HGF, SDF-1, and MMP-9 are involved in stress-induced human CD34+ stem cell recruitment to the liver, *J. Clin. Invest.* 112 (2003) 160–169.
- [17] T. Kinoshita, A. Miyajima, Cytokine regulation of liver development, *Biochim. Biophys. Acta* 1592 (2002) 303–312.
- [18] J. Wineman, K. Moore, I. Lemischka, C. Muller-Sieburg, Functional heterogeneity of the hematopoietic microenvironment: rare stromal elements maintain long-term repopulating stem cells, *Blood* 87 (1996) 4082–4090.
- [19] M. Nanno, M. Hata, H. Doi, S. Satomi, H. Yagi, T. Sakata, R. Suzuki, et al., Stimulation of in vitro hematopoiesis by a murine fetal hepatocyte clone through cell–cell contact, *J. Cell Physiol.* 160 (1994) 445–454.
- [20] H. Taniguchi, T. Toyoshima, K. Fukao, H. Nakauchi, Presence of hematopoietic stem cells in the adult liver, *Nat. Med.* 2 (1996) 198–203.
- [21] T. Watanabe, K. Nakagawa, S. Ohata, D. Kitagawa, G. Nishitai, J. Seo, S. Tanemura, et al., SEK1/MKK4-mediated SAPK/JNK signaling participates in embryonic hepatoblast proliferation via a pathway different from NF-kappaB-induced anti-apoptosis, *Dev. Biol.* 250 (2002) 332–347.
- [22] N. Uchida, T. Fujisaki, A.C. Eaves, C.J. Eaves, Transplantable hematopoietic stem cells in human fetal liver have a CD34(+) side population (SP) phenotype, *J. Clin. Invest.* 108 (2001) 1071–1077.
- [23] M.F. Pittenger, A.M. Mackay, S.C. Beck, R.K. Jaiswal, R. Douglas, J.D. Mosca, M.A. Moorman, et al., Multilineage potential of adult human mesenchymal stem cells, *Science* 284 (1999) 143–147.
- [24] T. Okuda, J. van Deursen, S.W. Hiebert, G. Grosveld, J.R. Downing, AML1, the target of multiple chromosomal translocations in human leukemia, is essential for normal fetal liver hematopoiesis, *Cell* 84 (1996) 321–330.
- [25] K. Shinoda, S. Mori, T. Ohtsuki, Y. Osawa, An aromatase-associated cytoplasmic inclusion, the “stigmoid body,” in the rat brain: I. Distribution in the forebrain, *J. Comp. Neurol.* 322 (1992) 360–376.
- [26] H.K. Mikkola, Y. Fujiwara, T.M. Schlaeger, D. Traver, S.H. Orkin, Expression of CD41 marks the initiation of definitive hematopoiesis in the mouse embryo, *Blood* 101 (2003) 508–516.

- [27] G.G. Wulf, K.L. Luo, M.A. Goodell, M.K. Brenner, Anti-CD45-mediated cytoablation to facilitate allogeneic stem cell transplantation, *Blood* 101 (2003) 2434–2439.
- [28] D. Guo, T. Fu, J.A. Nelson, R.A. Superina, H.E. Soriano, Liver repopulation after cell transplantation in mice treated with retrorsine and carbon tetrachloride, *Transplantation* 73 (2002) 1818–1824.
- [29] S. Gupta, P. Rajvanshi, E. Aragona, C.D. Lee, P.R. Yerneni, R.D. Burk, Transplanted hepatocytes proliferate differently after CCl₄ treatment and hepatocyte growth factor infusion, *Am. J. Physiol.* 276 (1999) G629–G638.
- [30] H.M. Hatch, D. Zheng, M.L. Jorgensen, B.E. Petersen, SDF-1 α /CXCR4: a mechanism for hepatic oval cell activation and bone marrow stem cell recruitment to the injured liver of rats, *Cloning Stem Cells* 4 (2002) 339–351.
- [31] Y. Sato, Y. Igarashi, Y. Hakamata, T. Murakami, T. Kaneko, M. Takahashi, et al., Establishment of Alb-DsRed2 transgenic rat for liver regeneration research, *Biochem. Biophys. Res. Commun.* 311 (2) (2003) 478–481.
- [32] Y. Kanazawa, I.M. Verma, Little evidence of bone marrow-derived hepatocytes in the replacement of injured liver, *Proc. Natl. Acad. Sci. USA* 100 (Suppl. 1) (2003) 11850–11853.
- [33] R.E. Schwartz, M. Reyes, L. Koodie, Y. Jiang, M. Blackstad, T. Lund, T. Lenvik, et al., Multipotent adult progenitor cells from bone marrow differentiate into functional hepatocyte-like cells, *J. Clin. Invest.* 109 (2002) 1291–1302.
- [34] Y. Jiang, B.N. Jahagirdar, R.L. Reinhardt, R.E. Schwartz, C.D. Keene, X.R. Ortiz-Gonzalez, M. Reyes, et al., Pluripotency of mesenchymal stem cells derived from adult marrow, *Nature* 418 (2002) 41–49.



Herbal medicine Sho-saiko-to (TJ-9) increases expression matrix metalloproteinases (MMPs) with reduced expression of tissue inhibitor of metalloproteinases (TIMPs) in rat stellate cell

Isao Sakaida^{a,*}, Koji Hironaka^a, Teruaki Kimura^b, Shuji Terai^a,
Takahiro Yamasaki^a, Kiwamu Okita^a

^aDepartment of Gastroenterology and Hepatology, Yamaguchi University, School of Medicine, Minami-Kogushi 1-1-1, Ube, Yamaguchi 755-8505, Japan

^bDepartment of Bioregulatory Function, Yamaguchi University, School of Medicine, Minami-Kogushi 1-1-1, Ube, Yamaguchi 755-8505, Japan

Received 14 April 2003; accepted 18 September 2003

Abstract

We have reported that Sho-saiko-to (TJ-9) prevents liver fibrosis in vivo. To gain further insights into the effect of TJ-9, the matrix metalloproteinases (MMPs)/tissue inhibitors of metalloproteinases (TIMPs) balance was examined. Hepatic stellate cells (HSCs) were isolated from male Wistar rats and cultured with TJ-9 (0–1000 µg/ml) on uncoated plastic dishes for 4 days. To elucidate the effects on the MMPs/TIMPs balance by TJ-9, quantitative analysis of type IV collagen-degrading activity, gelatin zymography and reverse zymography were carried out. Northern blot analysis was performed to determine the expression of MMP-2, 13 and TIMP-1 mRNAs. TJ-9 treatment resulted in dose-dependent upregulation of MMP-2, 13 mRNA and downregulation of TIMP-1 mRNA up to 500 µg/ml. Gelatin zymography, reverse zymography and quantitative analysis of type IV collagen-degrading activity confirmed that TJ-9 increased MMP-2 activity and prevented TIMP-1, 2 activities in a dose-dependent manner. SB203580 diminished the reduction of mRNA as well as the activity of TIMP-1 by TJ-9 and induction of mRNA as well as the activity of MMP-2. These results show that TJ-9 increased MMP-2, 13 activity with reduced TIMP-1, 2 activities on HSCs possibly via P38 pathway.

© 2004 Elsevier Inc. All rights reserved.

Keywords: Herbal medicine; Fibrosis; Signal transduction; Metalloproteinase; Tissue inhibitor of metalloproteinase

* Corresponding author. Tel.: +81-836-22-2241; fax: +81-836-22-2240.

E-mail address: sakaida@po.cc.yamaguchi-u.ac.jp (I. Sakaida).

Introduction

Hepatic stellate cells have now been clearly identified as the primary cellular source involved in the pathogenesis of liver fibrosis (Friedman, 1991). During the development of liver fibrosis, stellate cells undergo activation, a process characterized by increased cell proliferation, morphological transformation into myofibroblast-like cells and synthesis of excessive extracellular matrix components (Friedman, 1991). These cells are also able to synthesize enzymes, called matrix metalloproteinases (MMPs), which can degrade matrix proteins in the extracellular space. The activity of MMPs is carefully regulated by controlling their conversion from pro-enzymes to the catalytic form and by a family of specific inhibitors, called tissue inhibitors of metalloproteinases (TIMPs).

On the other hand, many studies of signal transduction are now underway. The MAPK family of protein kinases includes the extracellular signal-regulated kinases (ERKs) (Boulton et al., 1991) the c-Jun N-terminal kinase/stress-activated protein kinases (JNK/SAPKs) (Derijard et al., 1994; Kyriakis et al., 1994), and p38 (Han et al., 1994). The MAPK signaling pathway is a multistep phosphorylation cascade that transmits signals from the cell's surface to cytosolic and nuclear targets (Cohen, 1997). It has been suggested that not only do MAPKs serve as the signaling pathways production of MMPs (Esparza et al., 1999; Zeigler et al., 1999), but that they also participate in production of TIMPs (Li and Zafarullah, 1998; Eberhardt et al., 2000). However, the role of ERK, SAPK and p38 pathways in regulating production of MMPs and TIMPs by HSCs is not well known at present.

Many agents have been proposed for the prevention and treatment of fibrosis but no specific inhibitor of stellate cell activation has yet been developed.

TJ-9 has been reported, including by us, to prevent fibrosis via the inhibition of HSCs in different animal models of fibrosis due to choline-deficiency (Sakaida et al., 1998a,b), and pig serum (Shimizu et al., 1999), as well as in isolated stellate cells (Kayano et al., 1998). TJ-9, commonly prescribed in Japan as Sho-saiko-to, is the most popular herbal medicine in Japan and has been widely used in the treatment of chronic liver diseases, especially chronic viral hepatitis. TJ-9 consists of an aqueous extract from the roots of scutellaria, glycyrrhiza, bupleurum, and ginseng; the pinella tuber; the jujube fruit; and the thew ginger rhizome. A number of studies have indicated its cytoprotective effects in experimental liver injuries (Yamamoto et al., 1985; Araki et al., 1988), cancer-preventive effects (Okita et al., 1993, 1994; Tatsuta et al., 1991; Oka et al., 1995), anti-tumor, and apoptotic effects (Matsuzaki et al., 1996; Yano et al., 1994).

From the clinical point of view, treatment for liver fibrosis has been mainly focused on prevention of stellate cell activation instead of acceleration of degradation.

To gain further insights into the effect of TJ-9 on suppression of hepatic fibrosis, we examined changes of the MMPs/TIMPs balance and MAPK pathways of TJ-9 treated HSCs.

Materials and methods

Animals

Male Wistar rats weighting 400 to 450 g (Nippon SLC Co., Ltd., Shizuoka, Japan) were obtained, quarantined for 1 week, and housed in a room under controlled temperature (25 °C), humidity, and

lighting (12 hours light, 12 hours dark). Access to food and tap water was ad libitum. After a 1-week acclimation period on a basal diet (Oriental MF Diet; Oriental Yeast Company, Japan), the rats were used for the experiments.

Isolation and culture of rat hepatic stellate cells

Rat hepatic stellate cells (HSCs) were isolated with Nycodenz as described previously (Kayano et al., 1998).

Yields were $1.0\text{--}1.5 \times 10^7$ cells/rat. Cell viability was always over 95% as determined by the trypan blue exclusion test. Cell purity was more than 90% as assessed by the presence of yellow droplets and desmin immunoreactivity. Then isolated hepatic stellate cells were cultured at a density of 5.0×10^5 cells/ml in monolayer culture on uncoated 60-mm plastic dishes (Iwaki Glass Co., Ltd., Tokyo, Japan). All cultures were incubated at 37 °C in a humidified atmosphere of 5% CO₂ and 95% air. After incubation for 4 h, non-adherent cells were removed with a pipette and the culture medium was replaced with medium containing various concentrations of TJ-9 or medium alone (control). In some experiments, SB203580 or PD98059 (Calbiochem, La Jolla, CA) was added in addition to TJ-9. SB20380 and PD980597 were dissolved in DMSO at the final concentration of 0.1%. SB20238 is known as a highly specific inhibitor of p38 kinase (IC₅₀ = 34nM in vitro, 600 nM in cells) and even 100 μM does not significantly inhibit JNK and p42 MAP kinase, and PD98059 is known as specific inhibitor of ERK kinase (IC₅₀ = 2 μM), according to the manufacturer's instructions.

The medium was changed every 24 h and cell culture was continued up to 4 days (serum was depleted 24 h before the assessment).

The treated HSCs were scraped after being washed with PBS twice and suspended at 4 °C in 0.5 ml of PBS with 0.1% Triton X. An equal amount of total protein (100 μg) was applied for the quantitative analysis of type IV collagen-degrading activity, zymography and reverse zymography.

Preparation of culture medium with Sho-saiko-to (TJ-9)

Sho-saiko-to (TJ-9, powder) was kindly provided by Tsumura Co., (Tokyo, Japan). Water-soluble ingredients of TJ-9 were obtained as described previously (Kayano et al., 1998). The final concentrations of TJ-9 used were 10, 100, 500 and 1000 μg/ml. The PH values of all culture media with or without TJ-9 were adjusted to within the physiological range.

Hybridization probes

The following probes were used in this study. G3PDH (glyceraldehyde-3-phosphate dehydrogenase) (Sakaida et al., 1996, 1998a,b) was purchased from American Type Culture Collection (Rockville, MD, USA). TIMP-1 cDNAs was used as described (Sakaida et al., 1999). MMP-2 cDNA was a generous gift of Dr. Hiroshi Sato (Molecular Virology and Oncology, Cancer Research Institute, Kanazawa University, Ishikawa-Pref., Japan) (Sato et al., 1994). MMP-13 cDNA was the generous gift of Dr Cheryl O. Quinn (Pediatric Research Institute, Department of Pediatrics, Health Sciences Center, Saint Louis University, MO, USA) (Hironaka et al., 2000).

Northern blot analysis

Northern blot analysis was performed after the isolation of 10 µg of total RNA from isolated hepatic stellate cells as described previously (Hironaka et al., 2000). Each signal strength of mRNA was determined after normalization by relevant G3PDH mRNA levels.

Quantitative analysis of type IV collagen-degrading activity

Type IV collagen-degrading activity in conditioned media was determined as described previously (Hironaka et al., 2000) using a Type IV collagenase activity assay kit (YU-18001, Yagai Co., Kamagata, Japan). The principle of the type IV collagenase activity assay kit is based on fluorescent measurement of collagen fragments upon cleavage by gelatinases. It is known that collagen decomposition fragments differ from whole collagen in their temperature of denaturation and ethanol solubility. Upon gelatinase cleavage of fluorescently-labeled collagen type IV, decomposition fragments are produced. These fragments are selectively denatured and extracted with ethanol. The fluorescence intensity of the extracted product is measured and correlates with type IV collagen-degrading activity.

Zymography

As described by Durko et al. (Durko et al., 1997), SDS-polyacrylamide (10%) gels were copolymerized with gelatin at a final concentration of 1 mg/ml. The concentrated conditioned media were mixed 3:1 (v/v) with sample buffer (0.3 M Tris-HCl, pH 6.8, containing 8% SDS, 0.4% bromophenol blue and 40% glycerol), loaded onto the gels without boiling and separated by electrophoresis. The gels were washed for 1 h in a solution of 2.5% Triton X-100 in 40 mM Tris-HCl, pH 7.6, and for 15 min in 10 mM Tris-HCl, pH 8. For the enzymatic reaction to take place, the gels were incubated for 18 h at 37 °C in a solution of 50 mM Tris-HCl, pH 8, containing 10 mM CaCl₂. The gels were stained for 2 h in a 0.5% Coomassie blue R250 solution, then destained in 20% methanol with 10% acetic acid until clear bands (indicating lysis) were apparent on the blue background. Prestained molecular weight markers were resolved on the same gels, separated from other samples after electrophoresis and fixed in 5% acetic acid. To characterize the protease bands, some of the gels were incubated in a buffer (50 mM Tris-HCl, pH 8, with 10 mM CaCl₂) containing 20 mM EDTA (a metalloproteinase inhibitor).

Reverse zymography

Reverse zymography was performed as previously described (Herron et al., 1986). Gelatinase inhibitory activity was detected by incubating standard gelatin zymograms for 1 h at 37 °C in a preparation of purified collagenase (2 unit/ml) before incubation at 37 °C for 18 h in a solution of 50 mM Tris-HCl, pH 8, containing 10 mM CaCl₂. Gels were stained and destained as described above, after which stained bands manifested the presence of gelatinase inhibitory activity corresponding to TIMPs in the polyacrylamide gels.

Statistical analysis

Results are presented as the mean \pm SD. Statistical analysis was performed using Student's t-test and one-way analysis of variance (ANOVA). A p-value of less than 0.05 was considered to be statistically significant.

Ethical considerations

This experiment was reviewed by the Committee of Animal Experiment Ethics in Yamaguchi University School of Medicine and was carried out under the Guidelines for Animal Experiments in Yamaguchi University School of Medicine (No. 105) and Notification (No. 6) of the Japanese Government.

Results

Effects of TJ-9 on MMP-2, 13 and TIMP-1 mRNA expression of activated HSC

Messenger RNA expression was investigated by Northern blot analysis on day 4 after culture. Under control culture conditions (no treatment), HSCs expressed MMP-2, 13 and TIMP-1 mRNAs (Fig. 1A, 1B, lane 1). 500 μ g/ml of TJ-9 significantly elevated MMP-2 transcripts expressed at 3.1 kb and strikingly inhibited TIMP-1 mRNA expression (Fig. 1A, 1B, line 2). Expression of MMP-13 mRNA with stellate cells was dramatically reduced in a time-dependent manner after isolation. Although MMP-13 mRNA expression was not detected after 4-day culture, addition of 500 μ g/ml of TJ-9 increased MMP-13 mRNA expression to a detectable level, though it was still very weak (Fig. 1A, 1B). Reduction of type I procollagen mRNA expression could be reproduced with 500 μ g/ml of TJ-9 as previously reported (Kayano et al., 1998).

Morphologically, TJ-9 seemed to prevent the transformation to myofibroblast-like cells as previously reported (data not shown) (Kayano et al., 1998).

The doses up to 1000 μ g/ml of TJ-9 showed no cytotoxicity with cultured stellate cells.

Effects of TJ-9 on MMP-2 and TIMPs production by activated HSC

When serum-free conditioned media derived from HSCs were analyzed on polyacrylamide gels copolymerized with 1 mg/ml gelatin, the band of lysis was observed in the zymograms. These gelatinolytic activities were completely inhibited when the gels were incubated in the presence of 20mM EDTA (data not shown), indicating that they were mediated by metalloproteinases. TJ-9 conditioned media exhibited gelatinase activities in a dose-dependent manner on gelatin zymograms, seen mainly as a triplet with bands at molecular masses of 70, 66 and 62kDa (Fig. 2A). The 66 kDa gelatinase predominated, and the 62 kDa band was at the limit of detection. These bands migrated in the Mr 62-70 kDa region corresponding to the predicted molecular weights for MMP-2. The appearance of these bands was dependent on the concentration of TJ-9, and gelatinase activity reached a peak at the concentration of 500 or 1000 μ g/ml. Upregulation of MMP-2 production was also confirmed by quantitative measurement using the type IV collagen-degrading assay. Collagen IV